



Published in final edited form as:

Eur J Neurosci. 2005 February ; 21(3): 647–657. doi:10.1111/j.1460-9568.2005.03903.x.

Zinc accumulation after target loss: an early event in retrograde degeneration of thalamic neurons

Peter W. Land and Elias Aizenman

Department of Neurobiology and Center for Neuroscience, University of Pittsburgh School of Medicine, Pittsburgh, PA 15261, USA

Abstract

Accumulation of cytoplasmic zinc is linked with a cascade of events leading to neuronal death. In many *in vivo* models of zinc-induced cell death, toxic concentrations of synaptically released zinc enter vulnerable neurons via neurotransmitter- or voltage-gated ion channels. *In vitro* studies demonstrate, in addition, that zinc can be liberated from intracellular stores following oxidative stress and contribute to cell death processes, including apoptosis. Here we describe accumulation of intracellular zinc in an *in vivo* model of cell death in the absence of presynaptic zinc release. We focused on the lateral geniculate nucleus (LGN) because LGN neurons undergo apoptosis when separated from their target, the primary visual cortex (V1), and the LGN is mostly devoid of zinc-containing presynaptic terminals. Infant and adult rats and adult mice received unilateral ablation of V1, either by aspiration or kainate injection. One to 14 days later, brain sections were stained with selenium autometallography or fluorescently labeled to localize zinc, or stained immunochemically for activated caspase-3. V1 lesions led to zinc accumulation in LGN neurons in infant and adult subjects. Zinc-containing neurons were evident 1–3 days after aspiration lesions, depending on age, but not until 14 days after kainate injection. Zinc accumulation was followed rapidly by immunostaining for activated caspase-3. Our data indicate that like neurotrauma and excitotoxicity, target deprivation leads to accumulation of zinc in apoptotic neurons. Moreover, zinc accumulation *in vivo* can occur in the absence of presynaptic zinc release. Together these findings suggest that accumulation of intracellular zinc is a ubiquitous component of the cell death cascade in neurons.

Keywords

apoptosis; kainate; lateral geniculate nucleus; rodent; target deprivation

Introduction

In vivo studies of neuronal injury following global ischemia (Tonder *et al.*, 1990; Koh *et al.*, 1996), trauma (Suh *et al.*, 2000) or seizures (Frederickson *et al.*, 1989; Riba-Bosch & Perez-Clausell, 2004) have implicated cytotoxic elevations of intraneuronal Zn^{2+} in the pathophysiology of neurodegeneration (Choi & Koh, 1998). In these models, a high concentration of Zn^{2+} is thought to be released from synaptic vesicles and enter vulnerable postsynaptic neurons via neurotransmitter- and voltage-gated ion channels (Weiss *et al.*, 1993; Koh & Choi, 1994; Sensi *et al.*, 1999). *In vitro* studies, however, clearly demonstrate that Zn^{2+} also can be liberated from intracellular stores and contribute to cell death processes, including apoptosis (Aizenman *et al.*, 2000). Thus, oxidative and nitrosative stressors liberate Zn^{2+} that normally is bound to cysteine residues of intracellular metalloproteins like metallothionein (MT, Pal *et*

al., 2004). Studies with cell-free assays demonstrate that redox agents such as 2,2'-dithiodipyridine (DTDP) can oxidize the cysteine residues of MT to release bound Zn^{2+} (Maret & Vallee, 1998). In neurons treated with DTDP, liberated Zn^{2+} can induce neuronal apoptosis via a p38 kinase-dependent process, requiring enhancement of Kv2.1-mediated potassium currents and caspase activation (McLaughlin *et al.*, 2001; Pal *et al.*, 2003). These findings strongly suggest that non-vesicular Zn^{2+} could have an important role in neurodegeneration, although *in vivo* conditions wherein Zn^{2+} -associated cell death occurs in the absence of presynaptic Zn^{2+} release are ill-defined.

It has long been known that destruction of cerebral cortical tissue leads to atrophy of specific thalamic nuclei (von Gudden, 1870). For example, damage to primary visual cortex (V1) results in death of projection neurons in the dorsal lateral geniculate nucleus (LGNd; Lashley, 1941; Matthews, 1973; Agarwala & Kalil, 1998a). It also has been observed that degeneration of thalamic neurons following cortical lesions occurs via apoptosis (Al-Abdulla *et al.*, 1998; Martin *et al.*, 2001; Al-Abdulla & Martin, 2002; Repici *et al.*, 2003), and may result from loss of trophic support after target removal (Eagleson *et al.*, 1990; Agarwala & Kalil, 1998b). Importantly, LGNd neurons, and the corticogeniculate neurons providing reciprocal feedback, do not sequester Zn^{2+} within their synaptic terminals (Garrett & Slomianka, 1992; Casanovas-Aguilar *et al.*, 1998). Indeed, the LGNd, like most principal thalamic nuclei, is nearly devoid of Zn^{2+} -containing synapses (Mengual *et al.*, 2001). We therefore used LGNd neurons and their trophic dependence on V1 as a model system for investigating the association of non-vesicular Zn^{2+} with the apoptotic cascade *in vivo*. Following damage to V1 by aspiration lesion or excitotoxic insult, staining for Zn^{2+} occurs in the cytoplasm of LGNd neurons, and this is followed rapidly by activation of caspase-3. These findings indicate that target deprivation, like ischemia, trauma and excitotoxicity leads to Zn^{2+} accumulation in dying neurons.

Materials and methods

Animal preparation

All procedures were performed in accordance with the National Institutes of Health 'Guide for the Care and Use of Laboratory Animals' and were approved by the University of Pittsburgh Institutional Animal Care and Use Committee. Long-Evans black-hooded rats (175–200 g), female rats with litters and C57/BL6 mice (17–25 g) were obtained from Harlan Sprague-Dawley (Indianapolis, IN, USA). Adult rats and mice, and postnatal day (P) 10 infant rats were anesthetized with tribromoethanol (232 mg/kg, *i.p.*) and placed in a stereotaxic device to stabilize the head. Under aseptic conditions, a midline scalp incision was made, and the skin and subcutaneous connective tissue over the right calvarium were reflected. For adult subjects a dental burr was used to make a 4 mm × 4 mm (rat) or 3 mm × 3 mm (mouse) square craniectomy over the right occipital cortex. The medial boundary of the craniectomy was located approximately 0.5 mm lateral to the sagittal suture; the caudal boundary was defined by the lambdoid suture. For P10 rats, a 3 mm × 3 mm craniectomy was made using a #11 scalpel blade to incise the cartilaginous skull. Dura mater was reflected using a 31 gage hypodermic needle and exposed cortical tissue was gently removed by subpial suction with a fire-polished Pasteur pipette (Fig. 1). The lesion cavity was extended ventrally until the alveus surface of the hippocampus was exposed. The location and extent of the lesion was intended to encompass most or all of primary visual cortex (V1; area 17) and adjacent secondary visual areas (Paxinos & Watson, 1986).

Some mice received, in addition, injections of kainic acid (KA) into the left occipital cortex in order to kill cortical neurons (the target of LGNd neurons) without damaging geniculocortical axons (Schwarcz & Coyle, 1977). This allowed us to compare in individual animals the effect of axotomy vs. target-deprivation *per se*. A 5 mM solution of KA in 0.9% sterile saline was loaded into glass micropipettes (tip diameter ~ 10 μ m). A craniectomy similar to that described

above was made over the left occipital cortex and the KA-containing micropipette was then inserted through the dura into the cortex to a depth of 0.5–1.0 mm. Approximately 0.2 μL of KA was injected at each site via pressure ejection (Picospritzer, General Valve, Fairfield, NJ, USA), and 20 such injections were made into the exposed cortex in a grid pattern with a center-to-center spacing of 0.5–1.0 mm. A small piece of Gelfoam (Upjohn, Kalamazoo, MI, USA) was placed over the lesion/injection site and the skin was closed with wound clips (adult rats) or with 6.0 sutures. All animals received 3 mg/kg Ketofen (ketoprofen; i.p.; Fort Dodge Animal Health, Fort Dodge, IA, USA), and upon recovering from anesthesia they were returned to their home cages where they remained for 24 h to 14 days.

Chelatable Zn^{2+}

Autometallographic (AMG) localization of Zn^{2+} in LGNd neurons was assessed using the selenium method described by Danscher (1982). Multi-element analyses based on particle-induced X-ray emission indicate that selenium precipitates in the mammalian brain stained by this procedure principally contain the metal ion Zn^{2+} (Danscher *et al.*, 1985). This technique previously has been shown to reveal synaptic Zn^{2+} as well as intracellular Zn^{2+} associated with neuronal cell death (Frederickson *et al.*, 1989). Animals received an i.p. injection of the Zn^{2+} chelator sodium selenite (20 mg/kg) from a freshly prepared stock solution (20 mg/mL in distilled H_2O) and were killed by decapitation 1 h later (see Table 1 for distribution of survival times by age and species). The brains were quickly removed, encased in OCT embedding medium (Miles, Elkhart, IN, USA) and rapidly frozen by surrounding them with crushed dry ice. Twenty-micron coronal sections through the brains were cut on a cryostat, collected onto warm (38 °C) microscope slides as a 1:3 series and stored with a desiccant at -40 °C until they were processed.

One series of sections through each brain was processed with AMG according to a modification of the Danscher method (Dyck *et al.*, 1993; Land & Akhtar, 1999). Briefly, slides were thawed, allowed to dry at room temperature, and fixed and hydrated in a descending series of ethanol (i.e. 95%, 15 min; 70%, 50%, 2 min each), after which they were rinsed in distilled H_2O (3×2 min). Slides were then dipped in 0.5% gelatin, dried and immersed in a physical developer prepared from 50% Acacia Gum (120 mL), 2.0 M sodium citrate buffer (20 mL), 0.5 M hydroquinone (30 mL) and 37 mM silver lactate (30 mL). The latter two reagents were added to the incubation medium in the dark. The slides were incubated in the dark for 90–180 min with agitation. After development, the slides were washed for 30 min in warm (40 °C) running tap water in order to remove gelatin and any adhering precipitates, then rinsed in distilled H_2O (3×2 min). The slides were fixed in 5% sodium thiosulphate for 12 min, rinsed in distilled H_2O (4×2 min) and postfixated in 70% alcohol for 30 min. Some section series were further dehydrated in ascending alcohols and coverslipped with Permount (Histologic Mounting Media, Fisher Scientific, FairLawn, NJ, USA). Other series were counterstained with 0.1% thionin or 1% acid fuchsin (Lees, 1989) after the AMG reaction to reveal degeneration-related changes in LGNd neurons, as well as to determine the cellular localization of silver staining.

Fluorescent Zn^{2+} detection

In some brains we visualized free Zn^{2+} using a fluorescent Zn^{2+} indicator, Zinpyr-1 (NeuroBioTex, Galveston, TX, USA), that became available during the course of this study. Zinpyr compounds were specifically developed to facilitate the visualization of intracellular Zn^{2+} in biological samples, and they exhibit strong fluorescence in response to nanomolar concentrations of Zn^{2+} in the presence of millimolar concentrations of Ca^{2+} and Mg^{2+} (Burdette *et al.*, 2003; Frederickson *et al.*, 2004a). Indeed, other common metal ions like Ca^{2+} , Mg^{2+} , K^+ and Na^+ elicit no appreciable change in the emission spectra of Zinpyr reagents (Frederickson *et al.*, 2004a). We did not repeat all experiments using Zinpyr, but the data confirm and extend our findings on cytoplasmic Zn^{2+} accumulation revealed by the AMG

method (see Results). Cryostat sections were prepared as above. Sections were immersed for 1–5 min in a 10 μ M solution of Zinpyr-1 prepared in 0.9% NaCl. Without rinsing, sections were coverslipped with glycerin and photographed under epifluorescence illumination. Coverglasses were removed, and the sections were washed in phosphate buffer containing 0.9% sodium chloride (phosphate-buffered saline, PBS; pH 7.3; 3×10 min) and fixed for 2 min in 4% paraformaldehyde. After rinsing in PBS, sections were exposed to 4',6-diamidino-2-phenylindole (DAPI; 1: 1000; Sigma) for 1 min, rinsed in 0.1 M phosphate buffer and coverslipped again with glycerin.

Zn²⁺ visualization in dko7 cells

Metal response element (MRE)-binding transcription factor-1 (MTF-1)-deficient dko7 cells were a gift from W. Schaffner (ESBATEch, Zurich, Switzerland). Cells were grown in Dulbecco's modified Eagle's medium (DMEM) supplemented with 10% fetal bovine serum, 24 U/mL penicillin, 24 U/mL streptomycin and 2 mM L-glutamine, and transfected with the MTF-1 expression vector (pCMV-MTF-1-FLAG; a gift from G. Andrews, University of Kansas Medical Center, Kansas City, KS, USA) or a blank vector, as previously described (Hara & Aizenman, 2004). Briefly, cells were seeded onto 11-mm glass coverslips at a cell density of 3.5×10^4 cells/well in a 24-well plate. The next day dko7 cells were transfected with 1.5 μ g DNA using LipofectAMINE (Gibco/BRL). Twenty-four hours later cells were exposed to 100 μ M Zn²⁺ for 10 min in MEM (plus 0.01% bovine serum albumin and 25 mM HEPES). After exposure cells were incubated with MEM for 2.5 h, and subsequently with 6 μ M Zinpyr-1 in MEM for 5 min, fixed with 10% formaldehyde and mounted on microscope slides for visualization.

Activated caspase-3

To establish the temporal relationship between occurrence of intracellular Zn²⁺ and neuronal apoptosis following cortical ablation we prepared a parallel series of animals wherein we immunohisto-chemically localized activated caspase-3. Twenty-four hours to 14 days post-lesion (see Table 1), rats and mice were anesthetized with isoflurane (IsoFlo, Abbott Laboratories, North Chicago, IL, USA) and perfused transcardially with 4% paraformaldehyde in 0.1 M sodium phosphate buffer (pH 7.3). Brains were removed, postfixed overnight then transferred to 30% sucrose in phosphate buffer for cryoprotection. Frozen sections were cut in the coronal plane at 30 μ m on a sledge microtome and collected in phosphate buffer. A 1: 3 series of sections was washed in PBS and preincubated for 1 h at room temperature in blocking serum (Blotto) consisting of PBS, 4% W/V non-fat dry milk and 0.4% Triton X-100. Sections were then incubated for 18 h at 4 °C in primary antisera from one of several sources directed against activated caspase-3, diluted in Blotto (BioVision, Mountain View, CA, USA, 1: 100 dilution; Cell Signalling Technology, Beverly, MA, USA, 1: 250 dilution; Merck-Frosst, Montreal, Quebec, Canada, 1: 16 000 dilution). Blocking peptide (e.g. the large fragment of activated caspase-3 resulting from cleavage) was used to test antibody specificity. Sections subsequently were washed 3×10 min in Blotto and transferred to Blotto containing biotinylated secondary antisera (1: 200; Vector Laboratories, Burlingame, CA, USA) for 1 h at room temperature. Sections then were washed in 0.1 M phosphate buffer and incubated in the Avidin/Biotin peroxidase complex (Vector) according to the manufacturer's instructions. After rinsing 3×10 min in phosphate buffer, sections were incubated in 0.5 mg/mL 3,3'-diaminobenzidine tetrahydrochloride (DAB) with 0.01% H₂O₂. In some cases (see below), nickel sulphate (2.5% W/V) was included in the reaction mixture to produce a black reaction product. DAB-stained sections were washed in phosphate buffer, mounted onto slides, dehydrated and coverslipped. Some series also were counterstained with 0.1% thionin.

Glial fibrillary acidic protein (GFAP)

During the course of this study we noted a relatively sparse 'background' immunostaining of cell nuclei throughout the brains of control and lesioned rats with all of the antibodies against activated caspase-3 (see also below). The comparatively small and consistent size of most stained nuclei suggested that they were non-neuronal. To test this we stained brain sections with anti-caspase-3 antibodies as described above, using nickel sulphate in the DAB step. After extensive washing in buffer (3×30 min) we then double-stained the sections with antibodies to GFAP, a marker for astroglial cells. Primary antisera (Polysciences, Warrington, PA, USA) were used at a dilution of 1: 8000. Remaining steps were as described above except that nickel sulphate was not included in the DAB reaction.

Data analysis

To characterize the time-course of Zn^{2+} accumulation in the LGNd we determined the number of Zn^{2+} -containing cells per unit area at different post-lesion survival times. We selected from each Zn^{2+} -stained brain a section at the rostrocaudal midpoint of the LGNd ipsilateral to cortical lesion and used Neurolucida (Microbrightfield, Williston, Vermont, USA) to measure the cross-sectional area of the nucleus. We then used the *Meander Scan* function to plot the location of Zn^{2+} -containing cells and calculate their number per mm^2 . In all cases there were no Zn^{2+} -containing cells in the LGN contralateral to cortical lesions (Figs 1 and 2).

We observed a low level of activated caspase-3 immunostaining in LGNd of rats ipsilateral and contralateral to cortical lesion at all survival times (e.g. Fig. 4). Such 'background' staining indeed was observed throughout each brain, was limited to the nuclear region of a small proportion of cells, and was completely blocked by preincubation of primary antiserum with immunizing peptide. As we show below, many of these nuclei appear to be associated with astroglial cells. Following cortical ablation there was a visible increase in the number of caspase-immunoreactive elements. In particular, this included the occurrence of cytoplasmic immunostaining in LGNd neurons following cortical lesions (see Results). However, in the absence of double-immunostaining, there was some ambiguity whether an individual stained element could be attributed to 'background' staining or to lesion-induced caspase activation. Thus, to characterize the time-course of activated caspase-3 expression, and to account for the potential presence of background immunostaining, we used Neurolucida as above to determine the number of immunoreactive elements per unit area in matched section through the LGNd ipsilateral *and* contralateral to cortical lesion. The data then are expressed as a ratio of IPSI/CONTRA labeling.

Results

Intracellular Zn^{2+} accumulates in apoptotic neurons

We used subpial aspiration of occipital cortex, including V1 and surrounding cortical areas, in P10 rats to induce degeneration of neurons in the ipsilateral LGNd and to investigate the association of cytoplasmic Zn^{2+} with the cell death process (Fig. 1A). This procedure previously was shown to result in rapid apoptotic loss of LGNd neurons (Cunningham *et al.*, 1979; Repici *et al.*, 2003). The LGNd, like most thalamic nuclei, has very low levels of chelatable Zn^{2+} , and somata of LGNd neurons normally do not contain free Zn^{2+} that can be revealed by AMG or other methods (Fig. 1B). By contrast, ablation of occipital cortex quickly leads to accumulation of chelatable Zn^{2+} within the cytoplasm of LGNd neurons whose cortical target was removed (Fig. 1C). Punctate staining within LGNd neurons can be detected by 24 h after cortical damage at P10, and is persistently observed in the LGNd for up to 5 days post-lesion, by which time a majority of neurons have degenerated (see also Cunningham *et al.*, 1979).

Chelatable Zn^{2+} in the LGNd ipsilateral to the ablated cortex is closely associated with other hallmarks of neuronal damage. For example, acid fuchsin counterstaining of sections processed with AMG reveals numerous acidophilic cells in the affected LGNd, most of which also contain chelatable Zn^{2+} (Fig. 2A and B). Silver deposits are largely coextensive with the cytoplasmic acidophilia of the axotomized neurons (i.e. Fig. 2B). Intracellular Zn^{2+} staining similarly is observed within cells exhibiting nuclear condensation, or pycnosis (Fig. 2C and D). In Nissl-stained sections, a cloud of silver-stained puncta typically surrounds the small, darkly stained nucleus obscuring other cellular detail (Fig. 2D). Chelatable Zn^{2+} thus accumulates in the cytoplasm of LGNd cells that are dead or are dying as a result of neonatal cortical lesion.

Time-course of Zn^{2+} accumulation vs. caspase-3 activation

Recent studies indicate that visual cortex ablation in adult rats and mice also results in apoptosis of LGNd neurons (Al-Abdulla *et al.*, 1998; Martin *et al.*, 2001; Al-Abdulla & Martin, 2002), although over a longer time-course than in neonatal animals (Repici *et al.*, 2003). To evaluate the possible association of intracellular Zn^{2+} accumulation and cell death in adult LGNd, and to establish the temporal relationship between accumulation of cytoplasmic Zn^{2+} and the apoptotic response of mature neurons to loss of their cortical target, we performed occipital cortical ablations in adult rats and mice (see also below). We then stained sections through the LGNd to visualize cellular Zn^{2+} , as above, or with immunohistochemistry for activated caspase-3, the main executioner protease in the apoptotic pathway in mammalian neurons (Kuida *et al.*, 1996).

Ablation of occipital cortex leads to accumulation of chelatable Zn^{2+} in the cytoplasm of mature LGNd neurons, as it does in neonatal neurons. In contrast with observations in infant rats, we first detected intracellular Zn^{2+} in mature neurons at 5 days post-lesion using autometallography. AMG staining can be observed in the affected LGNd for up to 14 days, the latest time point that we investigated (Fig. 3).

The apparently delayed onset of Zn^{2+} accumulation following adult vs. neonatal cortical lesions could reflect a reduced sensitivity of the AMG method in tissue from older animals. Alternatively, the time-course of Zn^{2+} accumulation may be modified as neurons mature. To address this in more detail we prepared several adult rats with cortical lesions, and stained sections through the LGNd with a recently developed high-affinity fluorescent Zn^{2+} indicator, Zinpyr-1 (Burdette *et al.*, 2003). Zinpyr-1 reveals a diffuse cohort of Zn^{2+} -containing cells in the LGNd and surrounding structures as early as 3 days post-lesion, but not at 1 or 2 days as we saw in infant rats (Fig. 4A and B). In confirmation of our AMG data, numerous labeled cells are seen at 5 days (Fig. 4C) and thereafter. Thus, in terms of Zn^{2+} accumulation, the cellular response to target loss is delayed by several days in adult compared with neonatal neurons, but nevertheless appears to begin somewhat earlier than what the AMG data reveal.

Notably, at 3 days post-lesion Zinpyr-1 staining is associated with cellular nuclei, a location that never is stained by the AMG method (Fig. 4D–F). At later survival times Zinpyr-1 also labels cytoplasmic Zn^{2+} , as does autometallography (Fig. 4G–I). This suggests an early response of LGNd cells to cortical damage that selectively targets Zn^{2+} to the cell nucleus, and a later response wherein Zn^{2+} accumulates in the cytoplasm. The early response could reflect Zn^{2+} binding by MTF-1, which is a selective intracellular Zn^{2+} sensor that rapidly translocates to the nucleus upon binding free cytoplasmic Zn^{2+} (Westin & Schaffner, 1988; Palmiter, 1994). To test whether Zinpyr-1 can reveal the presence of MTF-associated Zn^{2+} we transfected dko7 cells, derived from mouse embryos having homozygous knockout of the MTF-1 gene (Heuchel *et al.*, 1994), with either empty vector or with MTF-1 expression plasmid, and then challenged the cells with 100 μ M Zn^{2+} for 10 min. Whereas the nuclei of dko7 cells transfected with empty vector are relatively unstained 2.5 h following the Zn^{2+} exposure (Fig. 4J), nuclei of cells transfected with MTF-1 become intensely stained with

Zinpyr-1 following similar exposure conditions (Fig. 4K). This indicates that Zinpyr-1 can reveal Zn^{2+} that has been delivered to the nucleus as a result of MTF-1 translocation to that organelle.

In order to compare the time-course of zinc accumulation following cortex ablation with other components of the cell death cascade in this paradigm, we used immunohistochemistry for the cleaved, active form of caspase-3 to look for caspase activation in LGNd neurons. Activation of caspase-3, like accumulation of cytoplasmic Zn^{2+} , requires several days to become apparent in adult LGNd neurons ipsilateral to cortical damage. Antisera from several sources (see Materials and methods) produced sparse staining of cellular nuclei throughout the brains of operated and control rats (Fig. 5A and C). This 'background' nuclear staining, like the cytoplasmic staining described below, is completely blocked by preincubation of primary antisera with immunizing peptide (data not shown). Double-immunostaining with antisera against GFAP revealed that most stained nuclei are associated with astroglial processes (Fig. 5D). Caspase-3 expression within nuclei of astrocytes is not accompanied by chelatable zinc, as both the AMG and Zinpyr methods produce labeling only within the affected LGNd of operated subjects.

In addition to nuclear staining within astroglia, we could detect robust cytoplasmic labeling for cleaved caspase-3 in the LGNd ipsilateral to cortical damage beginning at 5 days after cortex ablation (Fig. 5B). Immunoreactivity for cleaved caspase-3 is observed within somata and neurites of what appear to be LGNd projection neurons (Fig. 5E). The number of caspase-3-immunoreactive cells increases for several days, with the highest numbers reached at about 7 days (Fig. 6). The number of caspase-3-immunoreactive cells declines somewhat thereafter, although stained elements still can be observed after 14 days survival, the latest time point we investigated.

Zn^{2+} -associated cell death results from target deprivation

To address whether intracellular Zn^{2+} accumulation and apoptotic cell death of LGNd neurons results from loss of cortically derived neurotrophic factors or other molecules essential for neuronal survival, or from direct mechanical injury of LGNd neurons we prepared a series of adult mice that received unilateral cortical ablation as above. Upon completion of the cortical lesion, the mice then received injections of KA into the opposite hemisphere to produce excitotoxic death of occipital cortical neurons without damaging LGNd axons (see Materials and methods; Schwarcz & Coyle, 1977).

Chelatable Zn^{2+} first can be detected in adult mouse LGNd cells ipsilateral to subpial cortex aspiration about 5 days after surgery, as described above for rats, and Zn^{2+} -containing cells can be detected there for at least 14 days (Fig. 7C, F and I). In the contralateral hemisphere that received cortical kainate injection the LGNd remains essentially free of AMG reaction product for at least 11 days (Fig. 7B and E). There also is little evidence of cortical degeneration around the injection sites until that time (compare Fig. 7A with D). However, 11–14 days after kainate injection occipital cortical tissue shows histological changes that include thinning of the cortical mantle and loss of Zn^{2+} staining associated with cortical intrinsic circuits in the area of injection (Fig. 7D and G; Garrett & Slomianka, 1992). Simultaneously, LGNd neurons in the injected hemisphere begin to contain chelatable Zn^{2+} (Fig. 7H). It seems likely therefore that expression of cytoplasmic Zn^{2+} is a prominent feature of a neuron's response to target deprivation *per se*.

Discussion

Zn²⁺ accumulation in dying LGNd neurons

Neurons in the mammalian LGNd atrophy and die if they are disconnected from their target, V1. Here we show that an early and consistent feature of neuronal degeneration in the developing and mature LGNd as a result of V1 ablation is accumulation of intracellular Zn²⁺ in affected neurons. The presence of Zn²⁺ in dying LGN cells was corroborated by two independent methods, each of which has high selectivity for the metal ion (Danscher *et al.*, 1985; Frederickson *et al.*, 2004a). Our results demonstrate that Zn²⁺ accumulates in LGNd neurons despite a paucity of Zn²⁺-containing presynaptic terminals in that nucleus, and is followed rapidly by activation of caspase-3. We also provide evidence that this Zn²⁺-associated neurodegeneration results from target deprivation, *per se*, and does not require direct damage to LGNd cells. Thus, accumulation of intracellular Zn²⁺ appears to be a ubiquitous and naturally occurring component of the cell death process in neurons (Pal *et al.*, 2004). Indeed, the elevation in the concentration of cytoplasmic Zn²⁺, in and of itself, may be an important trigger of the neurodegenerative process, as a large amount of evidence now supports the role of this metal in initiating a variety of cell death-inducing cascades in neurons (Koh, 2001; see also Frederickson *et al.*, 2004b).

Accumulation of intracellular Zn²⁺ and activation of caspase-3 in LGNd neurons observed in the present study parallel, and to some extent presage, other morphological and molecular sequelae that have been described in the LGNd following cortical damage. Based upon examination of Nissl-stained material, neurons in adult rat LGNd ipsilateral to cortex ablation appear unremarkable and indistinguishable from normal for the first 3 days after surgery (Agarwala & Kalil, 1998a; Al-Abdulla *et al.*, 1998). However, our findings using the fluorescent Zn²⁺ indicator Zinpyr-1 indicate that Zn²⁺ already is beginning to accumulate within neuronal nuclei at this survival time, in advance of any gross cytological changes. One possibility is that at about 3 days after injury Zn²⁺ is transported to the nucleus as a result of binding to the transcription factor MTF-1, from which it can be displaced by Zinpyr-1 but not by autometallography. Two days later, on the fifth post-lesion day, we observed both Zinpyr-1 stained and histochemically reactive Zn²⁺ throughout the cytoplasm of dying cells; Zn²⁺-containing cells were present until the end of the second week. This coincides with a period during which there is profound atrophy and loss of LGNd projection neurons following cortical ablation (Agarwala & Kalil, 1998a; Al-Abdulla *et al.*, 1998).

Increased immunostaining for the active (cleaved) form of caspase-3 in the ipsilateral vs. contralateral LGNd followed a similar, though temporally shifted, time-course compared with intracellular Zn²⁺ accumulation. Thus, the number of caspase-3-immunoreactive elements in the ipsilateral LGNd rose markedly above background on the fifth post-lesion day and continued to increase until 1 week after the lesion. The number of caspase-3-immunoreactive elements declined during the second post-lesion week, presumably due to death and removal of most LGNd projection neurons (Lashley, 1941; Matthews, 1973; Agarwala & Kalil, 1998a). These data are consistent with the findings of Martin *et al.* (2001) who showed that protein levels of pro-caspase-3 (i.e. the inactive pro-enzyme) are significantly elevated in soluble fractions of LGNd homogenates by 4 days after cortex ablation, which was followed by a peak in protein levels for the activated form of caspase-3 1 day later, at 5 days post-lesion. Moreover, levels of p53, a transcription factor that regulates expression of pro-apoptotic genes (Levine, 1997), and Bax, a pro-apoptotic regulatory protein (Deckwerth *et al.*, 1996), showed similar prominent increases between the fourth and fifth days following surgery (Martin *et al.*, 2001). Together these findings point to an earlier, upstream event, perhaps associated with Zn²⁺ accumulation, which leads to neurodegeneration in the LGNd after cortex ablation. Specifically, using Zinpyr-1 we were able to detect intracellular Zn²⁺ at 3 days post-surgery. This is 2 days prior to the detection of the active form of caspase-3 at 5 days. This sequence

parallels previous *in vitro* findings showing that oxidant-induced release of the metal from intracellular binding stores not only precedes but is required for caspase activation (McLaughlin *et al.*, 2002).

We also observed accumulation of cytoplasmic zinc in LGNd neurons of infant rats (i.e. P10–P14) following ablation of V1. In contrast with findings in adult rats, where we first detected intracellular Zn^{2+} after 3 days, numerous Zn^{2+} -containing cells already were evident in the LGNd of infant rats by 24 h post-lesion, the earliest time point examined with the histochemical technique. Interestingly, Repici *et al.* (2003) recently showed that caspase-3 activation in LGNd neurons of perinatal rats first can be detected 24 h after cortex lesion (though not earlier), with peak activation occurring at 2 days post-lesion, a finding we have confirmed in preliminary studies (Land & Aizenman, unpublished). There is therefore a close temporal relationship between accumulation of cytoplasmic Zn^{2+} and caspase activation in infant rats as there is in adults. The more rapid onset of these events in young animals may reflect a greater dependence of immature neurons on their synaptic targets (Jones & Lavell, 1986; see also Martin *et al.*, 1998).

Zn^{2+} accumulation is dependent on target deprivation

Degeneration of LGNd neurons following cortex ablation can be ameliorated by application of basic fibroblast growth factor, ciliary neurotrophic factor or conditioned medium from co-cultures of thalamic and cortical neurons to the region of the lesion cavity (Eagleson *et al.*, 1990, 1992; Agarwala & Kalil, 1998b). The neuroprotective effect of such agents suggests that LGNd cell death results from loss of specific trophic factors synthesized by cortical target neurons. Our results comparing effects of cortex ablation vs. cortical kainate injections, which kills cortical neurons without damaging axons of LGNd cells, support this idea. Both procedures led to Zn^{2+} accumulation in LGNd neurons, but in kainate-injected hemispheres the occurrence of cytoplasmic Zn^{2+} was delayed an additional week, coinciding with the time when cortical target neurons had degenerated. These findings further indicate that, like ischemia (Tonder *et al.*, 1990; Koh *et al.*, 1996), neurotrauma (Suh *et al.*, 2000) and excitotoxicity (Frederickson *et al.*, 1989; Choi & Koh, 1998; Riba-Bosch & Perez-Clausell, 2004), target deprivation leads to accumulation of Zn^{2+} in apoptotic neurons. Our findings suggest, however, that this phenomenon occurs even in the absence of a presynaptic source of vesicular zinc.

Accumulation of intracellular Zn^{2+} in the absence of Zn^{2+} -containing terminals

The fact that Zn^{2+} accumulates in dying LGNd neurons in the apparent absence of vesicular Zn^{2+} release adds to a growing body of evidence that Zn^{2+} from non-synaptic sources is associated with neuronal cell death (Aizenman *et al.*, 2000). For example, infusion of compounds that generate nitric oxide (NO) into cerebellar cortex, portions of which like the LGNd have very low levels of chelatable zinc, leads to intense Zn^{2+} staining in somata of Purkinje neurons (Frederickson *et al.*, 2002). NO, and NO-derived species, are potent liberators of Zn^{2+} from intracellular stores like MT and other Zn^{2+} -containing proteins (Aravindakumar *et al.*, 1999; Pearce *et al.*, 2000; Pal *et al.*, 2004), and one possibility is that NO leads to increased cytoplasmic staining for Zn^{2+} by displacing it from protein binding sites. That non-vesicular Zn^{2+} is associated with neuronal cell death also is evident from studies of seizure-induced neuronal damage in mice with targeted disruption of the genes encoding the vesicular zinc transporter, ZnT-3, or MT. Thus, kainate-induced seizures in ZnT-3 null mice that lack synaptic vesicle zinc result in Zn^{2+} accumulation in degenerating hippocampal neurons, as it does in wild-type mice (Lee *et al.*, 2000). In this case cytoplasmic Zn^{2+} presumably is derived from non-synaptic sources. Kainate treatment also leads to Zn^{2+} -mediated neurodegeneration in thalamic nuclei that, as noted above, contain little or no synaptic zinc. Importantly, Zn^{2+} -associated thalamic cell death is nearly abolished in mice lacking the MT gene, strongly

suggesting that Zn^{2+} released from intracellular stores may be a critical contributor to the cell death process (Lee *et al.*, 2003). It remains to be determined, however, whether the cytoplasmic Zn^{2+} observed in all pathophysiological, slowly developing conditions like target deprivation is derived from MT itself, or other sources.

Our results suggest that accumulation of intracellular Zn^{2+} in thalamic neurons deprived of their cortical targets may be an early and critical sign of the impending demise of these cells. Based on earlier work, the accumulation of Zn^{2+} in neurons destined to die may be a reflection of the liberation of this metal from intracellular binding proteins following an oxidative or nitrosative signal (Aizenman *et al.*, 2000; Sensi *et al.*, 2003; Bossy-Wetzel *et al.*, 2004; Pal *et al.*, 2004). As target and growth factor deprivation-induced apoptosis models have implicated oxidative stress as an important component of the cell death cascade (Estevez *et al.*, 1998; Martin *et al.*, 2003; Pandey *et al.*, 2003), it is quite conceivable that a similar event has taken place in our LGNd model. What the sources of this oxidative signal are, or the mechanisms by which these signals are triggered in afflicted neurons are unclear at this time. Nonetheless, the newfound importance of non-synaptic Zn^{2+} sources as a trigger of neuronal cell death provides several novel targets in the ongoing, strategic battle against neurodegenerative processes in the brain (see also Frederickson *et al.*, 2004b).

Acknowledgments

We thank Lorraine Shamalla-Hannah and Karen Hartnett for most excellent technical assistance. The contribution of Giovanni Di Pino was not insignificant. This work was supported by NIH grant NS43277.

Abbreviations

AMG	autometallographic
DAB	3,3'-diaminobenzidine tetrahydrochloride
DAPI	4',6-diamidino-2-phenylindole
DMEM	Dulbecco's modified Eagle's medium
DTDP	2,2'-dithiodipyridine
GFAP	glial fibrillary acidic protein
KA	kainic acid
LGN	lateral geniculate nucleus
MT	metallothionein
MRE	metal response element
MTF-1	MRE-binding transcription factor-1
PBS	phosphate-buffered saline
V1	primary visual cortex

References

- Agarwala S, Kalil RE. Axotomy-induced neuronal death and reactive astrogliosis in the lateral geniculate nucleus following a lesion of the visual cortex in the rat. *J Comp Neurol* 1998a;392:252–263. [PubMed: 9512272]
- Agarwala S, Kalil RE. Long-term protection of axotomized neurons in the dorsal lateral geniculate nucleus in the rat following a single administration of basic fibroblast growth factor or ciliary neurotrophic factor. *J Comp Neurol* 1998b;392:264–272. [PubMed: 9512273]

- Aizenman E, Stout AK, Hartnett KA, Dineley KE, McLaughlin B, Reynolds IJ. Induction of neuronal apoptosis by thiol oxidation: putative role of intracellular zinc release. *J Neurochem* 2000;75:1878–1888. [PubMed: 11032877]
- Al-Abdulla NA, Martin LJ. Projection neurons and interneurons in the lateral geniculate nucleus undergo distinct forms of degeneration ranging from retrograde and transsynaptic apoptosis to transient atrophy after cortical ablation in the rat. *Neuroscience* 2002;115:7–14. [PubMed: 12401317]
- Al-Abdulla NA, Portera-Cailliau C, Martin LJ. Occipital cortex ablation in adult rat causes retrograde neuronal death in the lateral geniculate nucleus that resembles apoptosis. *Neuroscience* 1998;86:191–209. [PubMed: 9692754]
- Aravindakumar CT, Cuelemans J, De Ley M. Nitric oxide induces Zn²⁺ release from metallothionein by destroying zinc-sulphur clusters without concomitant formation of S-nitrosothiol. *Biochem J* 1999;344:253–258. [PubMed: 10548558]
- Bossy-Wetzel E, Talantova MV, Lee WD, Scholzke MN, Harrop A, Mathews E, Gots T, Han J, Ellisman MH, Perkins GA, Lipton SA. Crosstalk between nitric oxide and zinc pathways to neuronal death involving mitochondrial dysfunction and p38-activated K⁺ channels. *Neuron* 2004;41:351–365. [PubMed: 14766175]
- Burdette SC, Frederickson CJ, Bu W, Lippard SJ. ZP4, an improved neuronal Zn²⁺ sensor of the Zinpyr family. *J Am Chem Soc* 2003;125:1778–1787. [PubMed: 12580603]
- Casanovas-Aguilar C, Reblet C, Perez-Clausell J, Bueno-Lopez JL. Zinc-rich afferents to the rat neocortex: projections to the visual cortex traced with intracerebral selenite injections. *J Chem Neuroanat* 1998;72:97–109. [PubMed: 9719362]
- Choi DW, Koh JY. Zinc and brain injury. *Ann Rev Neurosci* 1998;21:347–375. [PubMed: 9530500]
- Cunningham TJ, Huddleston C, Murray M. Modification of neuron numbers in the visual system of the rat. *J Comp Neurol* 1979;184:423–433. [PubMed: 762291]
- Danscher G. Exogenous selenium in the brain: a histochemical technique for light and electron microscopic localization of catalytic selenium bonds. *Histochemistry* 1982;76:281–293. [PubMed: 6186642]
- Danscher G, Howell G, Perez-Clausell J, Herel N. The dithizone, Timms sulfide silver and the selenium methods demonstrate a chelatable pool of zinc in the CNS. A proton activation (PIXE) analysis of carbon tetrachloride extracts from rat brains and spinal cords intravitally treated with dithizone. *Histochemistry* 1985;83:419–422. [PubMed: 3000994]
- Deckwerth TL, Elliott JL, Knudson CM, Johnson EM Jr, Snider WD, Korsmeyer SJ. BAX is required for neuronal death after trophic factor deprivation and during development. *Neuron* 1996;17:401–411. [PubMed: 8816704]
- Dyck RH, Beaulieu C, Cynader M. Histochemical localization of synaptic zinc in the developing cat visual cortex. *J Comp Neurol* 1993;329:53–67. [PubMed: 8384221]
- Eagleson KL, Cunningham TJ, Haun F. Rescue of both rapidly and slowly degenerating neurons in the dorsal lateral geniculate nucleus of adult rats by a cortically derived neuron survival factor. *Exp Neurol* 1992;116:156–162. [PubMed: 1577123]
- Eagleson KL, Haun F, Cunningham TJ. Different populations of dorsal lateral geniculate nucleus neurons have concentration-specific requirements for a cortically derived neuron survival factor. *Exp Neurol* 1990;110:284–290. [PubMed: 2249738]
- Estevez AG, Spear N, Manuel SM, Radi R, Henderson CE, Barbeito L, Beckman JS. Nitric oxide and superoxide contribute to motor neuron apoptosis induced by trophic factor deprivation. *J Neurosci* 1998;18:923–931. [PubMed: 9437014]
- Frederickson CJ, Burdette SC, Frederickson CJ, Sensi SL, Weiss JH, Yin HZ, Balaji RV, Truong-Tran AQ, Bedell E, Prough DS, Lippard SJ. Method for identifying neuronal cells suffering zinc toxicity by use of a novel fluorescent sensor. *J Neurosci Meth* 2004a;139:79–89.
- Frederickson CJ, Maret W, Cuajunco MP. Zinc and excitotoxic brain injury: a new model. *Neuroscientist* 2004b;10:18–25. [PubMed: 14987444]
- Frederickson CJ, Cuajunco MP, Labuda CJ, Suh SW. Nitric oxide causes apparent release of zinc from presynaptic boutons. *Neuroscience* 2002;115:471–474. [PubMed: 12421613]
- Frederickson CJ, Hernandez MD, McGinty JF. Translocation of zinc may contribute to seizure-induced death of neurons. *Brain Res* 1989;480:317–321. [PubMed: 2713657]

- Garrett B, Slomianka L. Postnatal development of zinc-containing cells and neuropil in the visual cortex of the mouse. *Anat Embryol* 1992;186:487–496. [PubMed: 1443656]
- von Gudden B. Experimentaluntersuchungen über das peripherische und centrale Nervensystem. *Arch Psychiat Nervenkrank* 1870;2:693–723.
- Hara H, Aizenman E. A molecular technique for detecting the liberation of intracellular zinc in cultured neurons. *J Neurosci Meth* 2004;137:175–180.
- Heuchel T, Radtke F, Georgiev O, Stark G, Aguet M, Schaffner W. The transcription factor MTF-1 is essential for basal and heavy metal-induced metallothionein gene expression. *EMBO J* 1994;13:2870–2875. [PubMed: 8026472]
- Jones KJ, Lavelle A. Differential effects of axotomy on immature and mature hamster facial neurons: a time course study of initial nucleolar and nuclear changes. *J Neurocytol* 1986;15:197–206. [PubMed: 3723147]
- Koh JY. Zinc and disease of the brain. *Mol Neurobiol* 2001;24:99–106. [PubMed: 11831557]
- Koh JY, Choi DW. Zinc toxicity on cultured cortical neurons: involvement of N-methyl-D-aspartate receptors. *Neuroscience* 1994;60:1049–1057. [PubMed: 7936205]
- Koh JY, Suh SW, Gwag BJ, He YY, Hsu CY, Choi DW. The role of zinc in selective neuronal death after transient global cerebral ischemia. *Science* 1996;272:1013–1016. [PubMed: 8638123]
- Kuida K, Zheng TS, Na S, Kuan C, Yang D, Karasuyama H, Rakic P, Flavell RA. Decreased apoptosis in the brain and premature lethality in CPP32-deficient mice. *Nature* 1996;384:368–372. [PubMed: 8934524]
- Land PW, Akhtar ND. Experience-dependent alteration of synaptic zinc in rat somatosensory barrel cortex. *Somatosens Motor Res* 1999;16:129–140.
- Lashley KS. Thalamocortical connection in the rat's brain. *J Comp Neurol* 1941;75:67–121.
- Lee J-Y, Cole TB, Palmiter RD, Koh J-Y. Accumulation of zinc in degenerating hippocampal neurons of ZnT3-null mice after seizures: evidence against synaptic vesicle origin. *J Neurosci* 2000;20(1–5):RC79. [PubMed: 10807937]
- Lee JY, Kim JH, Palmiter RD, Koh JY. Zinc released from metallothionein-iii may contribute to hippocampal CA1 and thalamic neuronal death following acute brain injury. *Exp Neurol* 2003;184:337–347. [PubMed: 14637104]
- Lees GJ. In vivo and in vitro staining of acidophilic neurons as indicative of cell death following kainic acid-induced lesions in rat brain. *Acta Neuropathol* 1989;77:515–624.
- Levine AJ. p53, the cellular gatekeeper for growth and division. *Cell* 1997;88:323–331. [PubMed: 9039259]
- Maret W, Vallee BL. Thiolate ligands in metallothionein confer redox activity on zinc clusters. *Proc Natl Acad Sci USA* 1998;95:3478–3482. [PubMed: 9520391]
- Martin LJ, Al-Abdulla NA, Bambrink AM, Kirsch JR, Sieber FE, Portera-Cailliau C. *Brain Res Bull* 1998;46:281–309. [PubMed: 9671259]
- Martin LJ, Kaiser A, Yu JW, Natale JE, Al-Abdulla NA. Injury-induced apoptosis in adult brain is mediated by p53-dependent and p53-independent pathways and requires Bax. *J Comp Neurol* 2001;433:299–311. [PubMed: 11298357]
- Martin LJ, Price AC, McClendon KB, Al-Abdulla NA, Subramaniam JR, Wong PC, Liu Z. Early events of target deprivation/axotomy-induced neuronal apoptosis in vivo: oxidative stress, DNA damage, p53 phosphorylation and subcellular redistribution of death proteins. *J Neurochem* 2003;85:234–247. [PubMed: 12641745]
- Matthews MA. Death of the central neuron: an electronmicroscopic study of thalamic retrograde degeneration following cortical ablation. *J Neurocytol* 1973;2:265–288. [PubMed: 9224491]
- McLaughlin B, Hartnett KA, Erhardt JA, Legos JJ, White RF, Barone FC, Aizenman E. Caspase 3 activation is essential for neuroprotection in preconditioning. *Proc Natl Acad Sci USA* 2002;100:715–720.
- McLaughlin B, Pal S, Tran MP, Parsons AA, Barone FC, Erhardt JA, Aizenman E. p38 activation is required upstream of potassium current enhancement and caspase cleavage in thiol oxidant-induced neuronal apoptosis. *J Neurosci* 2001;21:3303–3311. [PubMed: 11331359]

- Mengual E, Casanovas-Aguilar C, Perez-Clausell J, Gimenez-Amaya JM. Thalamic distribution of zinc-rich terminal fields and neurons of origin in the rat. *Neuroscience* 2001;102:863–884. [PubMed: 11182249]
- Pal S, Hartnett KA, Nerbonne JM, Levitan ES, Aizenman E. Mediation of neuronal apoptosis by Kv2.1-encoded potassium channels. *J Neurosci* 2003;23:4798–4802. [PubMed: 12832499]
- Pal S, He K, Aizenman E. Nitrosative stress and potassium channel mediated neuronal apoptosis: is zinc the link? *Pflugers Arch* 2004;448:296–303. [PubMed: 15024658]
- Palmiter RD. Regulation of metallothionein genes by heavy metals appears to be mediated by a zinc-sensitive inhibitor that interacts with a constitutively active transcription factor, MTF-1. *Proc Natl Acad Sci USA* 1994;91:1219–1223. [PubMed: 8108390]
- Pandey S, Lopez C, Jammu A. Oxidative stress and activation of proteasome protease during serum deprivation-induced apoptosis in rat hepatoma cells; inhibition of cell death by melatonin. *Apoptosis* 2003;8:497–508. [PubMed: 14601556]
- Paxinos, G.; Watson, C. *The Rat Brain in Stereotaxic Coordinates*. Academic Press; New York: 1986.
- Pearce LL, Gandley RE, Han W, Wasserloos K, Stitt M, Kanai AJ, McLaughlin MK, Pitt BR, Levitan ES. Role of metallothionein in nitric oxide signaling as revealed by a green fluorescent protein. *Proc Natl Acad Sci USA* 2000;97:477–482. [PubMed: 10618443]
- Repici M, Atzori C, Migheli A, Vercelli A. Molecular mechanisms of neuronal death in the dorsal lateral geniculate nucleus following visual cortex lesions. *Neuroscience* 2003;117:859–867. [PubMed: 12654338]
- Riba-Bosch A, Perez-Clausell J. Response to kainic acid injections: changes in staining for zinc, FOS, cell death and glial response in the rat forebrain. *Neuroscience* 2004;125:803–818. [PubMed: 15099693]
- Schwarcz R, Coyle JT. Striatal lesions with kainic acid: neurochemical characteristics. *Brain Res* 1977;127:235–249. [PubMed: 16686]
- Sensi SL, Ton-That D, Sullivan PG, Jonas EA, Gee KR, Kaczmarek LK, Weiss JH. Modulation of mitochondrial function by endogenous Zn²⁺ pools. *Proc Natl Acad Sci USA* 2003;100:6157–6162. [PubMed: 12724524]
- Sensi SL, Yin YZ, Carriedo SG, Rao SS, Weiss JH. Preferential Zn²⁺ influx through Ca²⁺-permeable AMPA/kainate channels triggers prolonged mitochondrial superoxide production. *Proc Natl Acad Sci USA* 1999;96:2414–2419. [PubMed: 10051656]
- Suh SW, Chen JW, Motamedi M, Bell B, Listiak K, Pons NF, Danscher G, Frederickson CJ. Evidence that synaptically-released zinc contributes to neuronal injury after traumatic brain injury. *Brain Res* 2000;852:268–273. [PubMed: 10678752]
- Tonder N, Johansen FF, Frederickson CJ, Zimmer J, Diemer NH. Possible role of zinc in the selective degeneration of dentate hilar neurons after cerebral ischemia in the adult rat. *Neurosci Lett* 1990;109:247–252. [PubMed: 2330128]
- Weiss JH, Hartley SL, Koh JY, Choi DW. AMPA receptor activation potentiates zinc neurotoxicity. *Neuron* 1993;10:43–49. [PubMed: 7678965]
- Westin G, Schaffner W. A zinc-responsive factor interacts with a metal-regulated enhancer element (MRE) or the mouse metallothionein-I gene. *EMBO J* 1988;7:3763–3770. [PubMed: 3208749]

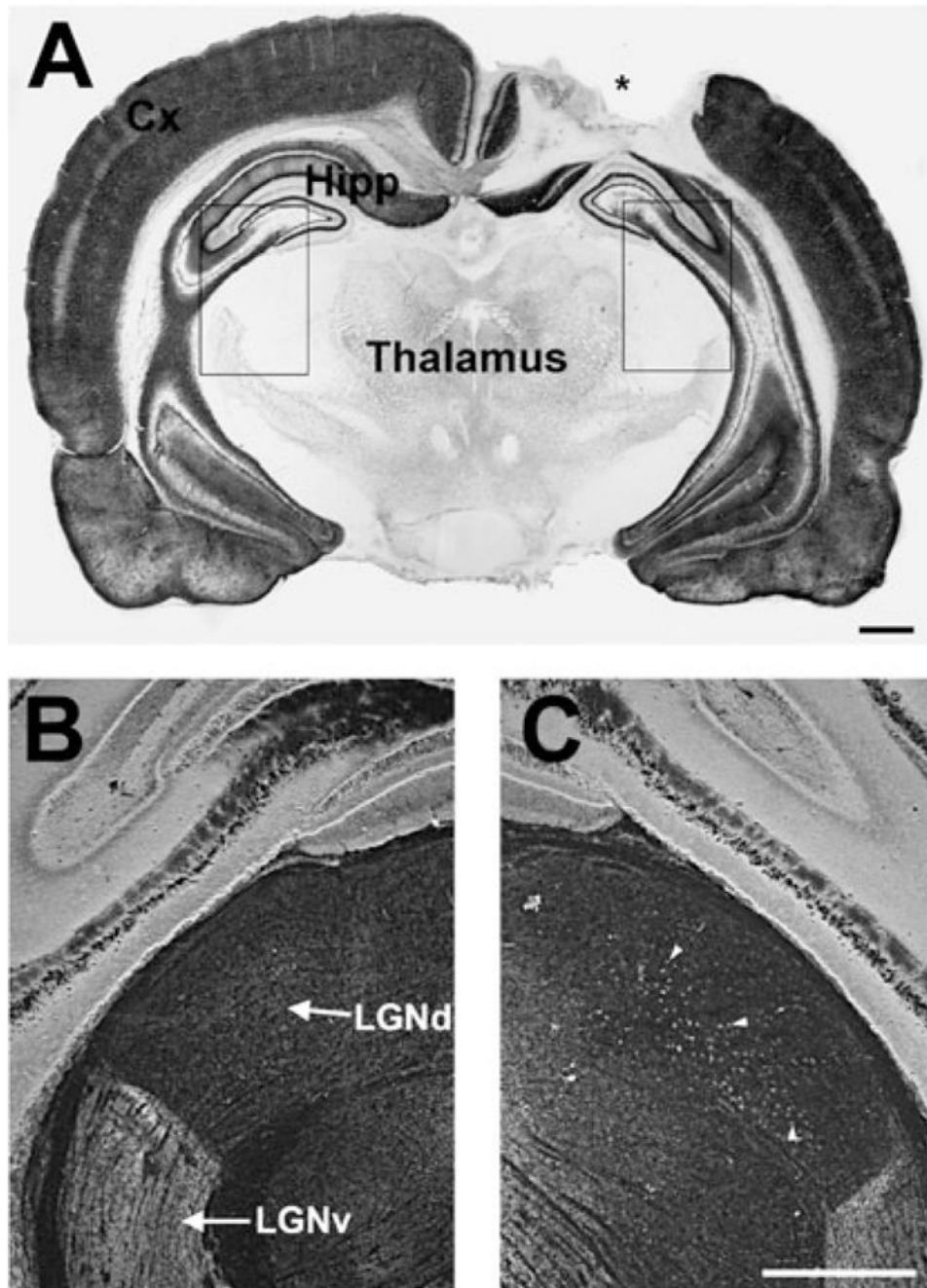


Fig. 1. Zn^{2+} accumulates in thalamic neurons after cortical lesion. (A) Coronal brain section from P12 rat stained histochemically for Zn^{2+} , which appears dark in this brightfield photomicrograph. Two days earlier, on P10, the rat sustained an aspiration lesion of visual cortex and surrounding areas (asterisk). Cortex (Cx) and hippocampus (Hipp) contain high levels of synaptic zinc and stain darkly. Thalamus and other subcortical structures have low levels of zinc staining. Boxed regions encompass the lateral geniculate nuclei and are shown at higher magnification in B and C. (B and C) Darkfield photomicrographs of boxed regions in (A) showing, respectively, the dorsal (LGNd) and ventral lateral geniculate nuclei (LGNv) contralateral (B) and ipsilateral (C) to the cortical aspiration. In both hemispheres the LGNv contains low-level Zn^{2+} staining

(bright in this darkfield photomicrograph) compared with the overlying hippocampus. The LGNd contralateral to the lesion (B) is essentially devoid of staining, whereas the ipsilateral LGNd (C) has numerous Zn^{2+} -containing cells (e.g. white arrowheads). Scale bars, 1 mm (A) and 300 μm (in C for B and C).

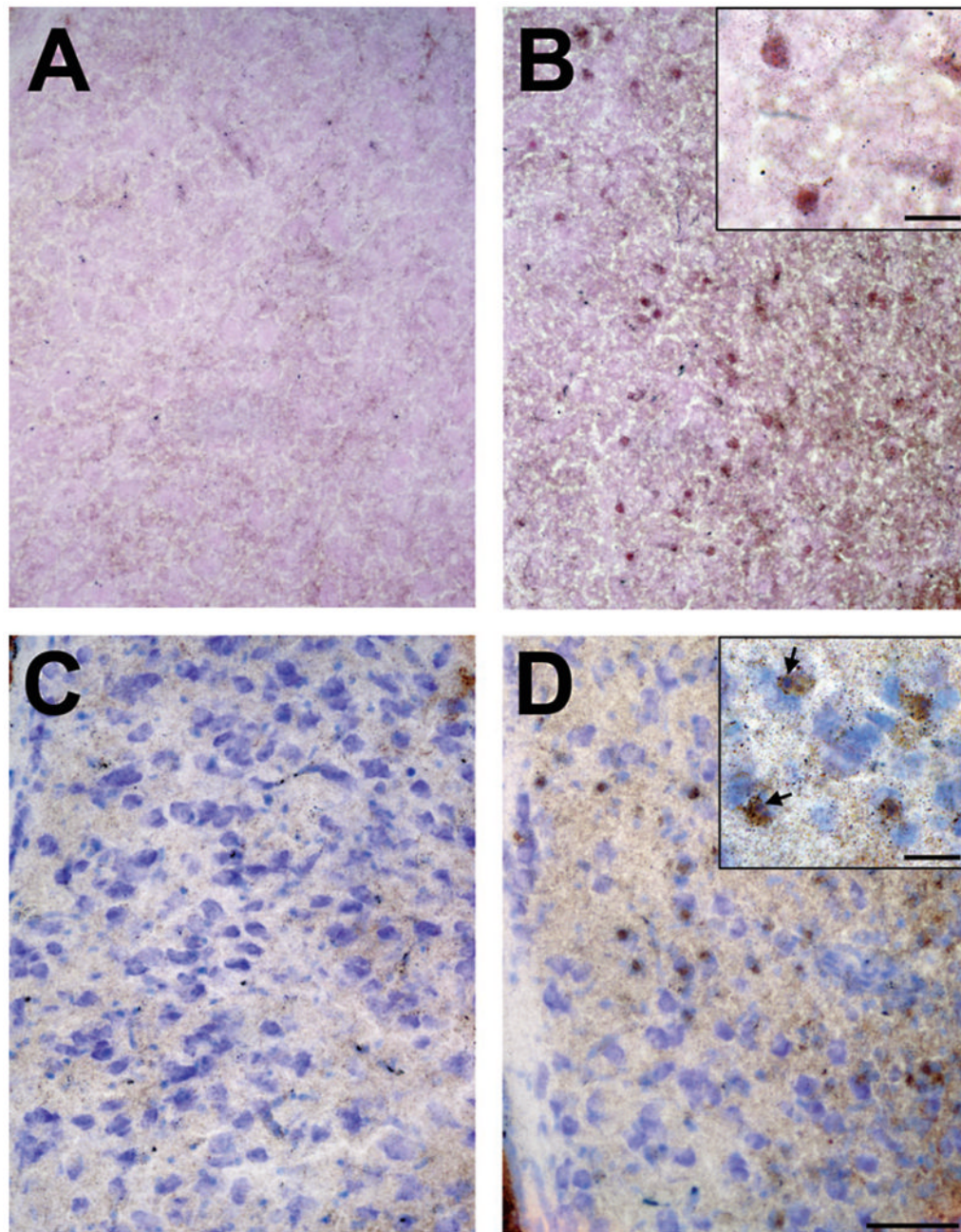


Fig. 2. Zn^{2+} is contained within dead or dying cells. (A and B) Sections through LGNd contralateral (A) and ipsilateral (B) to visual cortex lesion that were stained histochemically for Zn^{2+} and counterstained with acid fuchsin. Note only faint background staining in nucleus contralateral to cortical lesion (A). The ipsilateral LGNd (B) contains numerous cells with acidophilic cytoplasm, a hallmark of neuronal injury, that are associated with deposits of histochemically reactive Zn^{2+} . Inset shows several acidophilic/zinc-stained cells at higher magnification. (C and D) Sections through LGNd contralateral (C) and ipsilateral (D) to visual cortex lesion that were stained histochemically for Zn^{2+} and counterstained with thionin. Note normal Nissl appearance of LGNd neurons contralateral to cortical lesion (C). The ipsilateral nucleus (D) contains numerous zinc-stained cells. Inset shows that many of these cells exhibit darkly

stained, pycnotic nuclei (e.g. black arrows). Sections illustrated in (A–D) are from P14 rats that sustained cortical lesions on P10. Scale bar in D, 50 μm (for A–D); scale bars in insets, 20 μm .

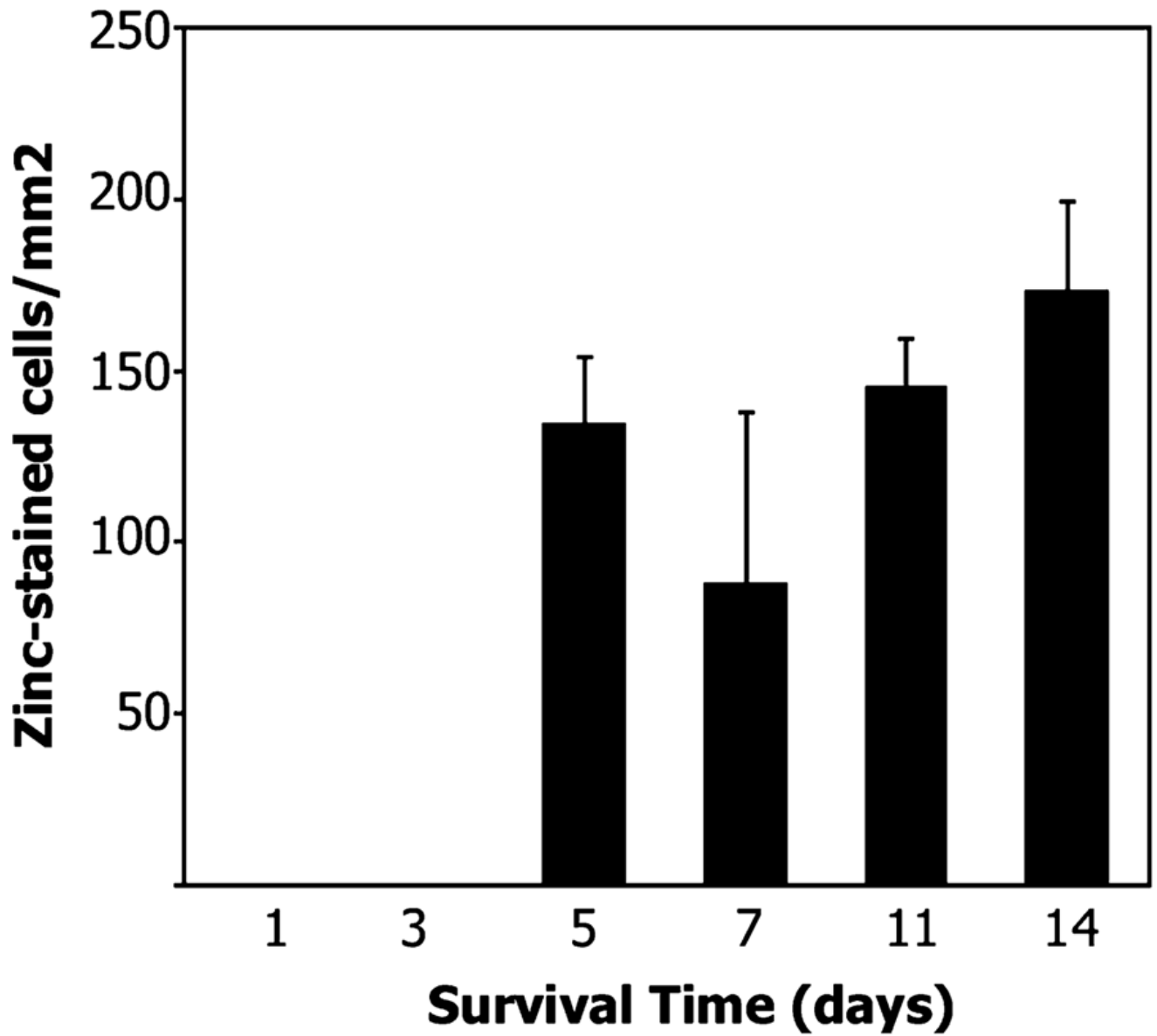


Fig. 3. Occurrence of histochemically reactive Zn^{2+} in adult LGNd. The chart shows the number of Zn^{2+} -containing cells per mm^2 revealed by histochemistry in adult LGNd at sequential time points following ablation of ipsilateral V1. The LGNd is devoid of Zn^{2+} histochemical staining until 5 days after surgery, at which time numerous Zn^{2+} -containing cells can be identified.

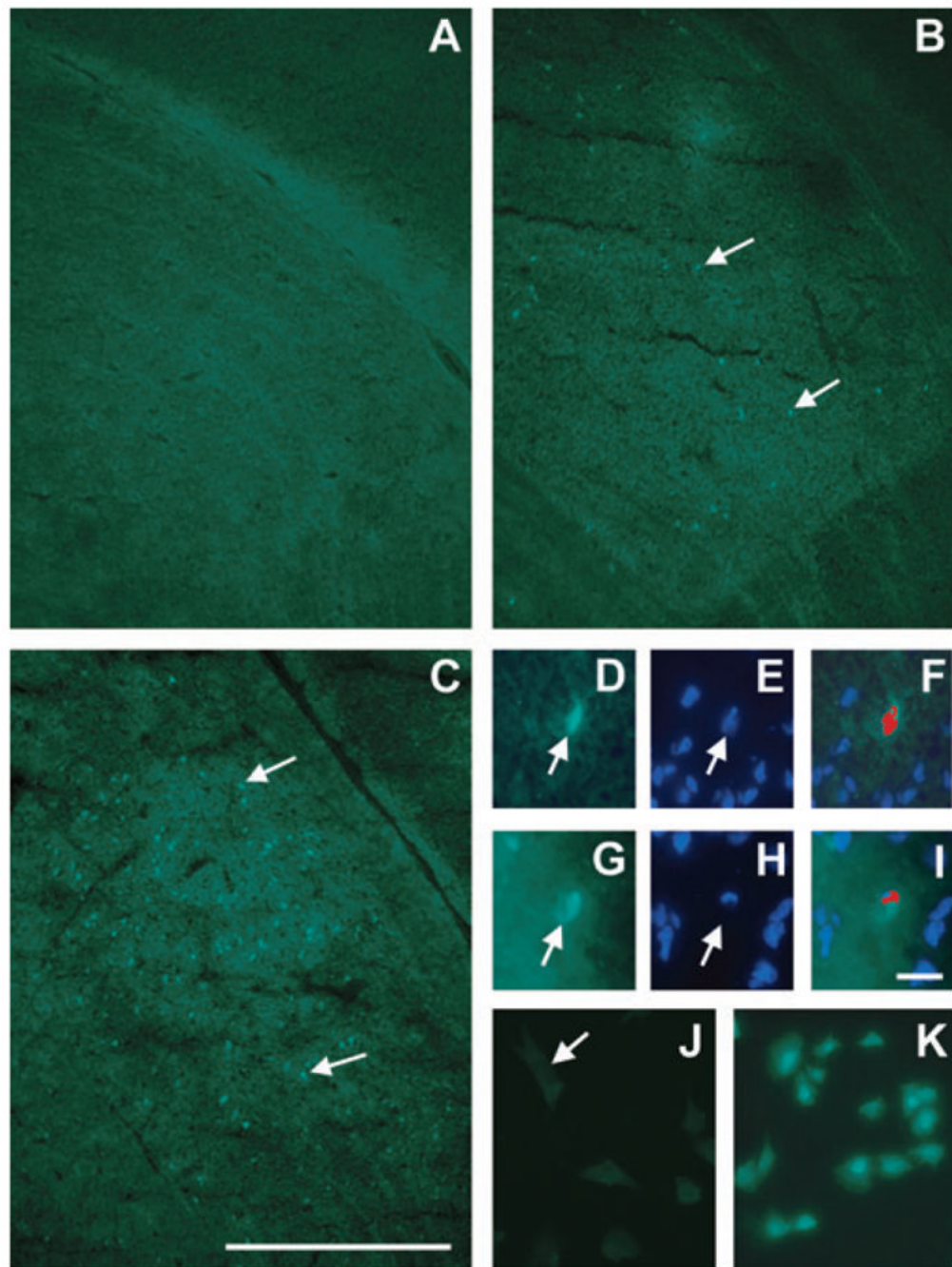


Fig. 4. Zn^{2+} accumulates sequentially in nuclear and cytoplasmic compartments. (A–C) Zinpyr-1 staining in lateral geniculate nucleus at, respectively, 2 days, 3 days and 5 days after ipsilateral visual cortex lesion in adult rats; arrows indicate brightly fluorescing elements, which are first detected at 3 days. (D–F) Zn^{2+} primarily is restricted to cell nuclei at 3 days post-lesion, as shown by double-labeling Zinpyr-1-stained elements (D) with DAPI (E); overlap of DAPI/Zinpyr-1 staining is rendered red in the overlay in F. Arrows are positioned at the same location in D and E. (G–I) In addition to its location in neuronal nuclei, which are somewhat shrunken at later survival times, Zn^{2+} also is present in the cytoplasm at 5 days post-lesion as shown by double-labeling for Zinpyr-1 (G) and DAPI (H); red in overlay (I) indicates overlap of Zinpyr-1/

DAPI signal. (J and K) Zinpyr-1 labeling of dko7 cells transfected with empty vector (J) or with MTF-1 construct (K), after exposure to 100 μM Zn^{2+} . Whereas cells without MTF-1 exhibit no nuclear staining with Zinpyr-1 (arrow in J), nuclei in MTF-1-transfected cells are strongly labeled with Zinpyr-1. Scale bars, 200 μm (in C for A–C) and 20 μm (in I for D–I).

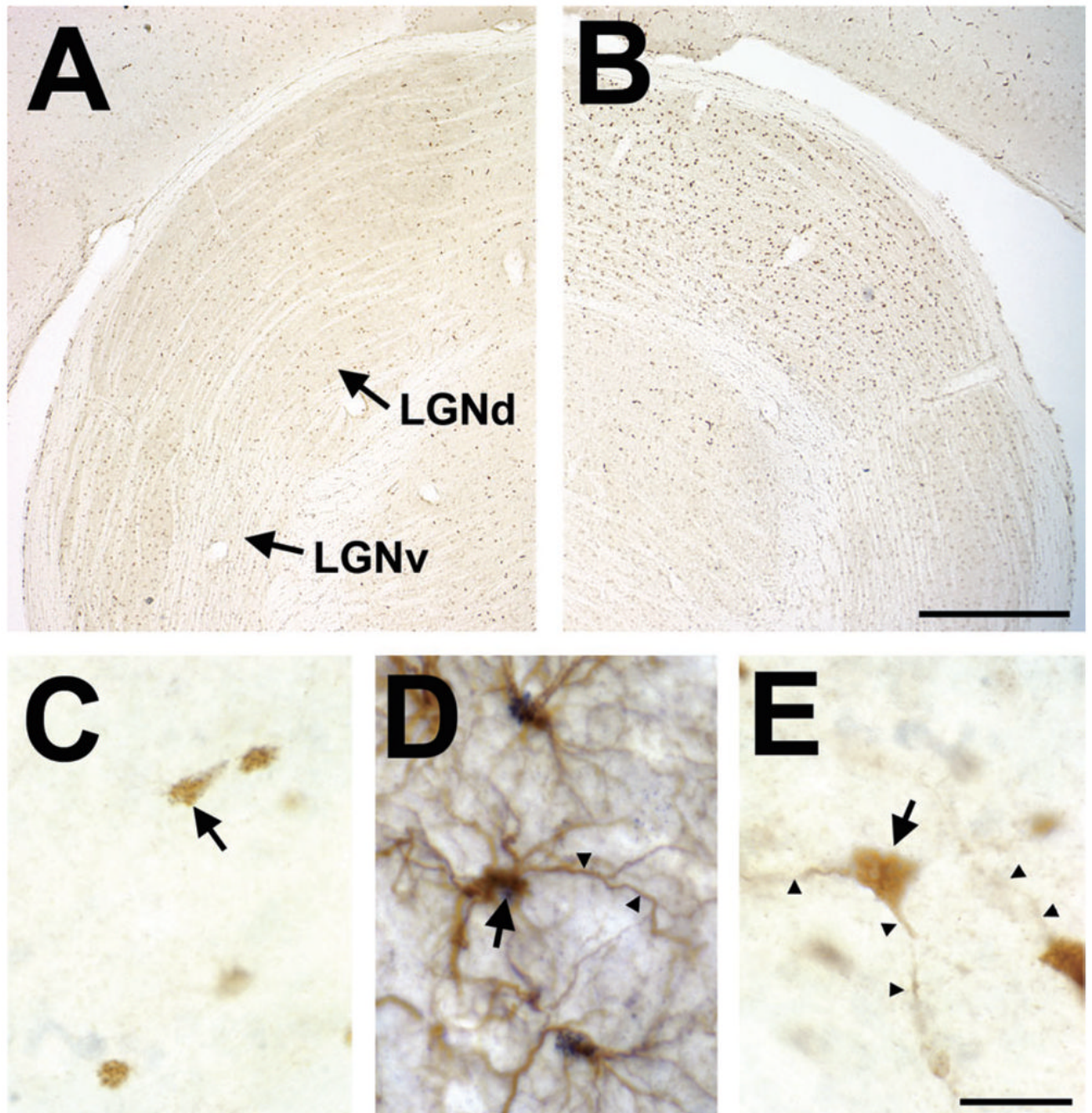


Fig. 5. Caspase-3 is activated in LGNd neurons after visual cortex lesion. (A and B) Sections through rat LGNd contralateral (A) and ipsilateral (B) to visual cortex lesion that were stained immunohistochemically for cleaved caspase-3. Only background staining is seen in the contralateral thalamus (A). In contrast, numerous darkly stained cells are present in the ipsilateral LGNd at 5 days after cortex lesion (B). The ipsilateral LGNv, which lacks a cortical projection, has only background staining. (C) Sparse pattern of nuclear staining (e.g. black arrow) is seen throughout the brain of control and operated rats, including within the LGNd contralateral to cortex lesion shown here. (D) Caspase-immunoreactive nuclei (e.g. black arrow) are associated with GFAP-immunoreactive astroglial processes (e.g. arrowheads).

Ipsilateral to cortex lesion (E) activated caspase-3 immunoreactivity appears in somata (e.g. black arrow) and processes (e.g. arrowheads) of LGNd neurons. Scale bars, 300 μm (in B for A and B) and 20 μm (in E for C–E).

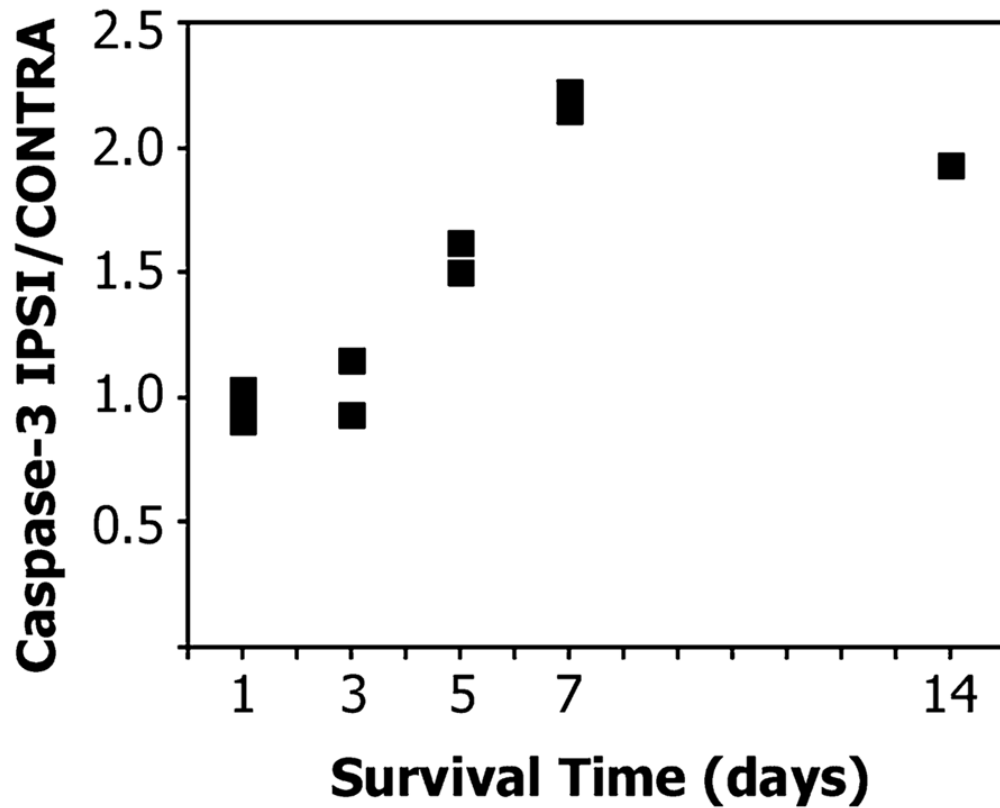


Fig. 6.

Time-course of caspase-3 activation after visual cortex lesion. Scatter plot compares the number of caspase-3-immunoreactive profiles in the LGNd ipsilateral to cortex lesion with that in the contralateral nucleus. All caspase-immunoreactive profiles were counted in the middle section in a rostro-caudal series through both LGNd of rats with unilateral V1 ablation (see Table 1) and a labeling index was calculated by dividing the number of labeled profiles in the ipsilateral nucleus by the number in the contralateral nucleus (i.e. the Ipsi/Contra ratio).

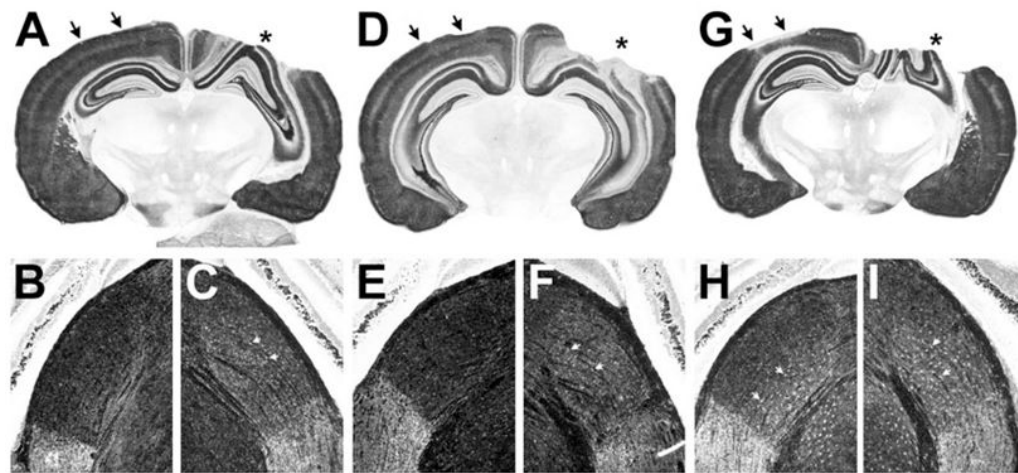


Fig. 7.

Kainate-induced cortical damage leads to Zn²⁺ accumulation in thalamic neurons. (A, D, G) Coronal brain sections stained histochemically for Zn²⁺ from mice subjected to V1 ablation (i.e. asterisk) and kainate injections (i.e. arrows) in opposite hemispheres 5 days (A), 11 days (B) or 14 days (G) before being killed. Note kainate-induced cortical damage is detectable at 11 days, and advanced by 14 days post-injection (arrows in D and G). Lower panels show paired, dark-field photomicrographs of the LGNd from each hemisphere. Zn²⁺-containing cells (e.g. white arrows) are present in the LGNd ipsilateral to V1 ablation at all survival times (C, F and I). In contrast, Zn²⁺-containing cells are not seen in the LGNd ipsilateral to kainate injection until about 14 days post-injection (H), by which time the cortex is in an advanced stage of degeneration (e.g. G).

Table 1

Distribution of experimental subjects

Animal group	Survival in days, and number (<i>n</i>)			
	Zn ²⁺ histochemistry, cortex ablation	Zn ²⁺ histochemistry, KA injection	Caspase immunostaining, cortex ablation	Zinpyr-1 staining, cortex ablation
P10 rats				
	1 day (5)	–	–	–
	2 days (5)	–	–	–
	3 days (4)	–	–	–
	4 days (6)	–	–	–
	5 days (1)	–	–	–
Adult rats				
	1 day (2)	–	1 day (3)	1 day (2)
	2 days (2)	–	3 days (2)	2 days (2)
	3 days (3)	–	5 days (2)	3 days (2)
	4 days (3)	–	7 days (3)	5 days (2)
	5 days (3)	–	14 days (3)	
	6 days (1)	–	–	–
	7 days (3)	–	–	–
	11 days (3)	–	–	–
	14 days (3)	–	–	–
Adult mice *				
	4 days (2)	4 days (2)	–	–
	5 days (2)	5 days (2)	–	–
	7 days (2)	7 days (2)	–	–
	11 days (2)	11 days (2)	–	–
	14 days (2)	14 days (2)	–	–

* These mice had cortex ablation and KA injection in opposite hemispheres.